# ENVIRONMENTAL SCIENCE

第 45 卷 第 5 期 2024 年 5 月 15 日

# 目 次

基于时间序列分解的京津冀区域 PM <sub>2.5</sub> 和 O <sub>3</sub> 空间分布特征····································	)
基于随机森林的北京城区臭氧敏感性分析 周红, 主鸣, 柴文轩, 赵昕(2497)	)
基于随机森林模型的四川盆地臭氧污染预测	
海口市臭氧浓度统计预报模型的构建与效果评估	
京津冀地区 2015~2020年 臭氧浓度时空分布特征及其健康效益评估高冉,李琴,车飞,张艳平,祖永刚,刘芬(2525)	
2022年北京市城区 PM <sub>2.5</sub> 水溶性离子含量及其变化特征 ····································	
郑州市冬春季 PM2.5 中金属元素污染特征、来源及健康风险评估	_
淄博市供暖前后PM <sub>2.5</sub> 中多环芳烃及其衍生物污染特征、来源及健康风险 孙港立,吴丽萍,徐勃,高玉宗,赵雪艳,姬亚芹,杨文(2558)	
西安市采暖季过渡期高时间分辨率细颗粒物组分特征及来源解析李萌津,张勇,张倩,田杰,李丽,刘卉昆,冉伟康,王启元 (2571)	_
天津冬季两个典型污染过程高浓度无机气溶胶成因及来源分析卢苗苗, 韩素芹, 刘可欣, 唐晓, 孔磊, 丁净, 樊文雁, 王自发 (2581)	
基于空间尺度效应的山东省PM2.5浓度时空变化及空间分异地理探测 ······徐勇,韦梦新,邹滨,郭振东,李沈鑫(2596)	
我国典型化工行业 VOCs 排放特征及其对臭氧生成潜势····································	
廊坊秋季大气污染过程中VOCs二次气溶胶生成潜势及来源分析张敬巧,刘铮,丁文文,朱瑶,曹婷,凌德印,王淑兰,王宏亮(2622)	)
景观格局对河流水质影响的尺度效应 Meta 分析	)
白洋淀夏季汛期入淀河流水体溶解性有机物的光谱特征及来源	,
一盆佳靖,窦红,陈哲,周石磊,底怡玲,武辰彬,王晨光,张家丰,崔建升(2640)	)
北京市丰台区永定河以东浅层地下水水化学演变规律及成因分析胡昱欣,周瑞静,宋炜,杨全合,王鑫茹(2651)	
郑庐断裂带(安徽段)浅层地下水水化学特征、控制因素及水质评价刘海,魏伟,宋阳,徐洁,管政亭,黄健敏,赵国红(2665)	)
农药施用对兴凯湖水中农药残留的影响及其风险评价王蔚青、徐雄、刘权震、林利华、吕婧、王东红(2678)	
黄河兰州段河岸带土壤中微生物与耐药基因的赋存特征 ····································	
基于多源数据的巢湖蓝藻水华时空分布及驱动因素分析金晓龙,邓学良,戴睿,徐倩倩,吴月,范裕祥(2694)	)
再生水构建水环境中沉水植物附着细菌群落特征贺赟,李雪梅,李宏权,魏琳琳,姜春晖,姜大伟,李魁晓(2707)	)
水位波动和植被恢复对三峡水库消落带土壤原核微生物群落结构的交互影响梅渝,黄平,王鹏,朱凯(2715)	
银川市典型湖泊沉积物细菌群落结构及其对重金属的响应关系 蒙俊杰,刘双羽,邱小琮,周瑞娟(2727)	)
热水解时间对污泥厌氧消化系统微生物群落结构影响分析张舍,张涵,王佳伟,高金华,文洋,李相昆,任征然(2741)	)
市政污水中吗啡来源辨析邵雪婷,赵悦彤,蒋冰,裴伟,李彦莹,谭冬芹,王德高(2748)	)
滹沱河流域生态环境动态遥感评价	)
黄河流域生态系统服务价值时空演化及影响因素王奕淇,孙学莹(2767)	)
热水解时间对污泥厌氧消化系统微生物群落结构影响分析····································	)
贵州高原典型喀斯特县域生境质量时空演变及定量归因 ···········李月,冯霞,吴路华,罗光杰,罗红芬(2793) 2000~2021年黄土高原生态分区 NEP 时空变化及其驱动因子 ······························周怡婷,严俊霞,刘菊,王琰(2806)	)
2000~2021年黄土高原生态分区 NEP时空变化及其驱动因子 ·······························周怡婷, 严俊霞, 刘菊, 王琰 (2806)	)
基于SSP-RCP情景的黄土高原土地变化模拟及草原碳储量 ····································	)
京津冀城市群建设用地扩张多情景模拟及其对生态系统碳储量的影响武爱彬,陈辅国,赵艳霞,秦彦杰,刘欣,郭小平(2828)	)
西南岩溶区土地利用变化对团聚体稳定性及其有机碳的影响	
不同土地利用方式下土壤有机质分子组成变化的整合分析黄世威, 赵一锴, 朱馨雨, 刘贺雷, 刘姣姣, 陈稍, 陈佳永, 张阿凤 (2848)	)
基于改进麻雀搜索算法优化 BP 神经网络的土壤有机质空间分布预测 ······················胡志瑞, 赵万伏, 宋垠先, 王芳, 林妍敏 (2859)	)
不同有机物料施用对菜地磷累积和转化的影响 孙凯,崔玉涛,李顺晋,魏冰丽,王媛,杨宏博,王孝忠,张伟(2871)	)
集约化柑橘种植抑制土壤磷循环微生物活性周连吴,曾全超,梅唐英泽,汪明霞,谭文峰(2881)	)
控释掺混肥对麦玉轮作体系作物产量和温室气体排放的影响	
生物炭对黄绵土中NO5-N运移过程影响及模拟	)
生物炭对黄绵土中NO5-N运移过程影响及模拟白一茹,刘旭,张钰涵,张睿媛,马艳,王幼奇(2905)	)
中国农田土壤重金属污染分析与评价	)
城市土壤和地表灰尘重金属污染研究进展与展望王晓雨,刘思峰,杨祥梦,王碧莲,林锦阔,颜梦霞,毕世杰 (2926)	)
场地重金属污染土壤固化及 MICP技术研究进展 ····································	)
黄河流域山东段近河道煤矿区土壤重金属污染特征及源解析戴文婷,张晖,吴霞,钟鸣,段桂兰,董霁红,张培培,樊洪明(2952)	)
拒马河流域河流沉积物与土壤重金属含量及风险评价韩双宝,袁磊,张秋霞,郑焰,李甫成 (2962)	
银川市黄河滩区土壤重金属污染特征、生态风险评价与来源解析于路加,马海军,王翠平(2971)	)
基于源导向和蒙特卡洛模型的广东省某城市土壤重金属健康风险评估	
·····································	)
西南典型碳酸盐岩高地质背景区农田重金属化学形态、影响因素及回归模型 … 唐瑞玲,徐进力,刘彬,杜雪苗,顾雪,于林松,毕婧(2995)	)
贵州省水田土壤-水稻 Hg 含量特征与安全种植区划 ······························韦美溜,周浪,黄燕玲,庞瑞,王佛鹏,宋波(3005)	
柠檬酸辅助甜高粱对南方典型母质土壤的镉修复效应 刘梦宇, 罗绪锋, 辜娇峰, 易轩韬, 周航, 曾鹏, 廖柏寒 (3016)	)
改性酒糟生物炭对紫色土壤镉形态及水稻吸收镉的影响肖乃川,王子芳,杨文娜,谢永红,代文才,高明(3027)	)
生物炭对四环素和铜复合污染土壤生菜生长及污染物累积的影响郑晨格,裴欢欢,张亚珊,李嘉欣,刘奋武,乔星星,秦俊梅(3037)	)
基于 Meta 分析的蚯蚓堆肥对堆肥质量和重金属的影响效应 ····································	)
微塑料对土壤 N,O 排放及氮素转化的影响研究进展	)
土地利用对洱海罗时江小流域土壤微塑料污染的影响戴柳云,侯磊,王化,符立松,王艳霞,李晓琳,王万宾,梁启斌(3069)	
养殖海湾淤泥质海岸沉积物微塑料污染特征 ************************************	
聚乙烯微塑料对盐渍化土壤微生物群落的影响王志超,李哲,李嘉辰,屈忠义,杨文焕,李卫平(3088)	)
鄱阳湖候乌栖息地微塑料表面细菌群落结构特征与生态风险预测。俞锦丽,赵俊凯,罗思琦,朱颖婷,张文慧,胡启武,刘淑丽(3098)	)
粤闽浙沿海重点城市道路交通节能减排路径徐艺诺, 翁大维, 王硕, 胡喜生, 王占永, 张园园, 张兰怡(3107)	
电动重卡替代柴油重卡的全生命周期碳减排效益分析	)

# 西安市采暖季过渡期高时间分辨率细颗粒物组分特征 及来源解析

李萌津1,2,张勇2,张倩1\*,田杰2,3,李丽2,刘卉昆2,冉伟康3,王启元2,3

(1. 西安建筑科技大学环境与市政工程学院,西安 710055; 2. 中国科学院地球环境研究所,西安 710061; 3. 陕西关中平原区域生态环境变化与综合治理国家野外科学观测研究站,西安 710061)

摘要: 受到供暖影响,北方城市秋冬季的大气细颗粒物( $PM_{2.5}$ )浓度升高,空气污染加剧.利用气溶胶化学组分监测仪、七波段黑碳仪以及大气多金属元素在线监测仪于 2019年 10月 25日至 11月 17日在西安市开展高时间分辨率  $PM_{2.5}$ 化学组分在线监测,分析采暖季过渡期  $PM_{2.5}$ 污染特征,同时结合正定矩阵因子分解模型解析  $PM_{2.5}$ 来源.结果表明,观测期间  $\rho(PM_{2.5})$ 平均值为  $(78.3\pm38.5)\mu g \cdot m^{-3}$ ,主要化学组分为有机物(OA)、二次无机离子(SIA)和粉尘,其占比分别为 38.7%、31.6%和 21.2%,其中  $\rho(SO_4^2 \cdot \Gamma)$ 、 $\rho(NO_5^2)$ 和 $\rho(NH_4^+)$ 平均值分别为 $(4.0\pm3.1)$ 、 $(14.9\pm13.7)$ 和 $(5.8\pm4.8)\mu g \cdot m^{-3}$ ,主要金属 $\rho(K)$ 、 $\rho(Ca)$ 和 $\rho(Fe)$  平均值分别为 $(1.0\pm0.4)$ 、 $(1.5\pm1.1)$ 和 $(1.4\pm0.9)\mu g \cdot m^{-3}$ ,BC(贡献率为 5.7%)、CF(贡献率为 1.3%)及微量元素(贡献率为 1.5%)对  $PM_{2.5}$ 的贡献率相对较低。在污染发展和维持阶段,OA和 SIA 浓度的增加幅度可达 137.7%~537.0%,在污染消散阶段则仅有粉尘浓度呈增长之势。来源解析结果显示二次源、生物质燃烧源、扬尘源、机动车源、工业源和燃煤源是观测期间  $PM_{2.5}$ 的主要来源,分别贡献了 29.1%、21.1%、15.3%、12.9%、11.4%和 10.2%,其中二次源和生物质燃烧源在污染发展和维持阶段贡献率较高,扬尘源在污染消散阶段贡献率较高。

关键词: 大气细颗粒物; 组分特征; 形成机制; 来源解析; 污染成因

中图分类号: X513 文献标识码: A 文章编号: 0250-3301(2024)05-2571-10 DOI: 10.13227/j. hjkx, 202306181

# Components Characteristic and Source Apportionment of Fine Particulate Matter in Transition Period of Heating Season in Xi'an with High Time Resolution

LI Meng-jin<sup>1,2</sup>, ZHANG Yong<sup>2</sup>, ZHANG Qian<sup>1\*</sup>, TIAN Jie<sup>2,3</sup>, LI Li<sup>2</sup>, LIU Hui-kun<sup>2</sup>, RAN Wei-kang<sup>3</sup>, WANG Qi-yuan<sup>2,3</sup>

(1. School of Environmental and Municipal Engineering, Xi'an University of Architecture and Technology, Xi'an 710055, China; 2. Institute of Earth Environment, Chinese Academy of Sciences, Xi'an 710061, China; 3. National Observation and Research Station of Regional Ecological Environmental Change and Comprehensive Management in the Guanzhong Plain, Xi'an 710061, China)

Abstract: Influenced by heating, the concentration of atmospheric fine particulate matter  $(PM_{2.5})$  rises in autumn and winter in northern cities. In this study, Q-ACSM, AE33, and Xact 625 were used to carry out online monitoring of  $PM_{2.5}$  chemical components with high time resolution in Xi'an from October 25 to November 17, 2019, to analyze the characteristics of  $PM_{2.5}$  pollution during the transition period of the heating season. Additionally, we analyzed the sources of  $PM_{2.5}$  in combination with the positive matrix factorization model. The results showed that the average  $PM_{2.5}$  concentration during the observation period was  $(78.3 \pm 38.5) \, \mu g^* m^{-3}$ , and the main chemical components were organic matter (OA), secondary inorganic ions (SIA), and dust, which accounted for 38.7%, 31.6%, and 21.2%, respectively. The average concentrations of sulfate, nitrate, and ammonium were  $(4.0 \pm 3.1)$ ,  $(14.9 \pm 13.7)$ , and  $(5.8 \pm 4.8) \, \mu g^* m^{-3}$ , and the average concentrations of the major metals potassium, calcium, and iron were  $(1.0 \pm 0.4)$ ,  $(1.5 \pm 1.1)$ , and  $(1.4 \pm 0.9) \, \mu g^* m^{-3}$ . Black carbon, chloride ions, and trace elements contributed relatively little to  $PM_{2.5}$  (5.7%, 1.3%, and 1.5%, respectively). In the pollution development and maintenance stage, the concentration of OA and SIA increased by 137.7% to 537.0%, whereas in the pollution dissipation stage, only the concentration of dust gradually increased. The source apportionment results showed that secondary sources, biomass burning, dust, vehicle emission, industrial emission, and coal combustion were the main sources of  $PM_{2.5}$  during the observation period, contributing 29.1%, 21.1%, 15.3%, 12.9%, 11.4%, and 10.2%, respectively. The contribution rate of secondary sources and biomass burning was higher in the pollution development and maintenance stage, and dust was higher in the pollution dissipation stage.

Key words: atmospheric fine particulate matter; components characteristics; formation mechanism; source apportionment; pollution causes

大气细颗粒物(PM<sub>25</sub>)对空气质量、气候变化以及人体健康产生不利影响,因而受到广泛关注<sup>[1-3]</sup>.在城市中,PM<sub>25</sub>主要通过化石燃料等人为源以及扬尘等自然源排放产生<sup>[4]</sup>.从秋季到冬季,我国北方城市中人为排放源将发生较大变化<sup>[5]</sup>,其原因在于11月温度降低,供暖开始,PM<sub>25</sub>浓度升高,从而加剧空气污染<sup>[6-8]</sup>.有研究表明,在采暖季的空气污染事件中,二次源以及生物质燃烧、燃煤等一次排放源是PM<sub>25</sub>的主要贡献者<sup>[9-11]</sup>.因此,不同城市的来源解

析工作将有利于当地政府减排措施的制订.

近年来,以高分辨率为优势的PM<sub>25</sub>化学组分在 线监测技术迅速发展,为PM<sub>25</sub>污染特征及来源的精

收稿日期: 2023-06-22; 修订日期: 2023-08-01

基金项目: 国家重点研发计划项目(2022YFF0802501);陕西省自然科学基础研究计划项目(2023-JC-JQ-23);陕西省自然科学基础研究计划项目(2022JQ-267);陕西省重点研发计划项目(2022ZDLSF06-07)

作者简介: 李萌津(1998~),男,硕士研究生,主要研究方向为大气颗

粒物来源解析,E-mail; limengjin1998@xauat. edu. cn \* 通信作者,E-mail; zhangqian2018@xauat. edu. cn 细化分析提供了重要的研究手段[12-14],并在污染事件成因分析中起着重要作用[15]. 在华北平原已有大量的使用在线监测仪器进行观测的研究,例如Pang等[16]对北京、天津和廊坊采暖季期间的区域传输和化学组分的形成机制进行探究. Yang等[8]发现区域传输、二次转化和沙尘暴是北京秋冬季发生极端雾霾事件的主要原因,其中硝酸盐的液相化学反应尤为重要. Han等[17]研究了天津冬季雾-霾的形成原因及PM25化学组分的变化. Liu等[12]结合多个模型分析了北京冬季典型污染事件演化过程中化学组分和来源的变化,并量化了区域传输的贡献. Lv 等[18]通过添加有机示踪剂将混合源细分,更利于分析京津冀地区雾-霾发生的原因.

汾渭平原具有以煤炭为主的高能耗、高排放的 能源结构, 且人口密度大、气象扩散条件不佳等特 点[19,20],导致该地区大气污染事件频发,特别是秋、 冬取暖季[21]. 为解决这一问题, 部分学者已在汾渭 平原的某些城市开展 PM25的来源解析工作,结果表 明二次源和燃煤源是该区域PM25的主要来源[21-24], 污染事件发生时二者贡献会迅速增加[23,24]. 西安位于 我国汾渭平原西南部,是空气污染最严重的地区之 25,26]. 由于城市化和工业化,能源消耗量和机动车 保有辆快速增长,西安面临着严重的高浓度PM25污 染问题[27]. 尽管近年来空气质量有所改善, 但秋冬 季不利的气象条件,易于PM25累积,仍容易引起污 染事件[28.29]. 目前关于西安市 PM2.5的相关研究主要集 中在冬季污染事件[28,30,31],对于采暖季过渡期污染 事件成因及来源的研究较为短缺.为此本研究于 2019年采暖季过渡期在西安开展 PM25在线监测, 获 得高时间分辨率化学组分特征,解析PM25来源,旨 在探索污染事件形成过程中组分及来源的高时间分 辨率演变规律.

#### 1 材料与方法

#### 1.1 站点描述

采样点位于陕西关中平原区域生态环境变化与综合治理国家野外科学观测研究站高新子观测场(34.13°N,108.52°E),周围主要是商业和住宅区,南侧有两个医药相关产业,东侧为唐延路及沣惠南路,车流量较大.在线监测设备包括气溶胶化学组分监测仪(Q-ACSM,美国Aerodyne公司)、七波段黑碳仪(AE33,美国Maggie公司)、大气多金属元素在线监测仪(Xact 625,美国Cooper环境服务公司),进样口距地面约10 m,取2019年10月25日至11月17日的数据进行分析.

#### 1.2 在线监测设备

 $PM_{25}$ 中有机物(OA)、硫酸根 $(SO_4^{2-})$ 、硝酸根 (NO;)、铵根(NH4\*)和氯离子(CI\*)组分浓度利用Q-ACSM 监测获取, 仪器分辨率约为15 min. 关于Q-ACSM 测量原理在其他相关研究里已经详细阐述[32]. 黑碳(BC)组分浓度数据通过AE33实时监测获取.简 单来说,AE33通过采样泵连续抽取含有气溶胶的样 气, 经采样管路后, 气溶胶沉积在带有特氟龙涂层 的玻璃纤维滤带上,根据BC在不同波段下对光的 吸收特性和透射光的衰减程度,获得不同波段下BC 浓度数据. 关于 AE33 的详细监测原理等内容参见文 献[33,34]. 无机元素组分浓度数据通过 Xact 625 获 取. Xact 625 基于 X 射线平台对环境气体中 25 种甚至 更多金属元素进行实时在线监测.简单来说环境空 气经过粒径切割器采样,样品沉积于滤带上,样品 前进至分析位置,使用X射线荧光法(XRF)分析样 品中的金属元素含量,并由数据处理软件计算得出 相应时段的浓度值[35,36]. 采样和分析同步连续进行, 提供连续的金属浓度数据.环境六参数和气象数据 分别从国家空气质量监测网(http://data.cma.cn/)和 气象监测网(http://www.weather.com.cn/)获取.

使用分析纯的 NH4NO3和(NH4)2SO4作为标准物质对 Q-ACSM 进行校准,其中 NH4NO3用于校准响应因子,NH4NO3和(NH4)2SO4分别用于获取 NO3和 SO4-的相对离子化效率;通过皂膜流量计对流量进行多次测定,并与进样口的压力进行线性回归,根据所得方程的斜率和截距对 Q-ACSM 的流量参数进行更新. AE33 日常校准的重点为流量校准和光学测试,其中流量校准需要使用流量计和流量校准膜,光学测试的结果偏差要小于10%.空白滤带测试、金属探棒测试和标准膜片校准是对 Xact 625 分析环节的质量控制,其中空白滤带测试是检查仪器的初始精密度偏差,除 K元素空白值偏高外其余元素均较低;内置探棒属于内标源测试,每日自动进行一次,数值偏差范围应低于5%;标准膜片校准则每3个月进行一次,用于保证仪器的准确可靠运行.

#### **1.3** 数据分析

#### 1.3.1 质量重构

 量元素浓度计算公式为: [微量元素] = [K]+[Cr]+ [Mn]+[Co]+[Ni]+[Cu]+[Zn]+[As]+[Se]+[Ba]+ [Pb]. 重构  $PM_{25}$ 质量浓度与附近国控站  $PM_{25}$ 在线监测质量浓度拟合结果显示,斜率和相关性分别为 0.98 和 0.88,表明此次观测数据具有一定的代表性.

#### 1.3.2 SOR和NOR计算

二次无机离子组分 $(SO_4^{2-},NO_3^{2}$ 和 $NH_4^{+},SIA)$ 通常对 $PM_{2.5}$ 质量浓度有较大贡献. $PM_{2.5}$ 中的SIA组分主要来自于前体物二次转化(SOR)和氮氧化率(NOR)来表征 $(SO_2)$ 及 $(NO_2)$ 的二次转化效率 $(SO_2)$ 2000年次,

$$SOR = \frac{n(SO_4^{2^-})}{n(SO_4^{2^-}) + n(SO_2)}$$
 (1)

$$NOR = \frac{n(NO_3^-)}{n(NO_3^-) + n(NO_2^-)}$$

$$to NEF ten + C.$$
(2)

#### 1.3.3 PM, 来源解析

正定矩阵因子分解(positive matrix factorization, PMF)模型是一种有效对颗粒物进行来源解析的数学受体模型,已成为我国该方面研究中最流行的手段之一<sup>[4]</sup>,模型原理和使用方法详细论述参见文献[43~45].模型输入组分浓度的不确定度计算方法如下,如果该组分浓度小于等于仪器检测限(MDL),则使用公式(3)进行计算.

$$Unc = \frac{5}{6} \times MDL \tag{3}$$

如果该组分浓度大于 MDL,则使用公式(4)进行计算.

Unc = 
$$\sqrt[2]{(10\% \times \text{concentration})^2 + (0.5 \times \text{MDL})^2}$$
(4)

PMF模型输入组分数据包括  $PM_{25}$ 、OA、 $SO_4^{2-}$ 、 $NO_3^{-}$ 、 $NH_4^{++}$ 、 $CI^{-}$ 、BC、Si、K、Ca、Cr、Mn、Fe、Co、Ni、Cu、Zn、As、Se、Ba、Pb在内的 21 种化学组分,将  $PM_{25}$ 设为总变量.为了确定最佳来源数量及解析结果,在  $5\sim7$ 因子之间进行了多次运行,综合考虑 Q值、残差、源谱及源贡献占比,最终确定 6个因子的解析方案为最优解.

#### 2 结果及讨论

#### 2.1 PM,5化学组分特征及形成

基于空气质量指数(AQI),本研究共识别 3 次污染事件(图 1),其选择标准为包含 AQI > 100 且至少持续 12 h的时间段.非污染期的定义为污染事件外剩余时间段.表 1 总结了不同时期  $PM_{25}$ 化学组分浓度特征.结果表明,整个采样期  $\rho(PM_{25})$ 在 6.9~167.8  $\mu$ g·m<sup>-3</sup>,平均值为(78.3 ± 38.5) $\mu$ g·m<sup>-3</sup>,其中 OA 是  $PM_{25}$ 的主要贡献者(贡献率为 38.7%),其次是

SIA(贡献率为 31.6%)和粉尘(贡献率为 21.2%).在 SIA中, $NO_3$ 的贡献最高[(14.9 ± 13.7) $\mu$ g·m<sup>-3</sup>],其次是  $NH_4$ <sup>+</sup>[(5.8 ± 4.8) $\mu$ g·m<sup>-3</sup>]和  $SO_4$ <sup>2</sup>-[(4.0 ± 3.1) $\mu$ g·m<sup>-3</sup>]. BC(贡献率为 5.7%)、CI<sup>-</sup>(贡献率为 1.3%)及微量元素(贡献率为 1.5%)对  $PM_{25}$ 贡献率相对较低.

如表 1 所示, 非污染期  $\rho(PM_{25})$  为 (66.5 ± 34.9) μg·m<sup>-3</sup>, 高于《环境空气质量标准》(GB 3095-2012)的一级标准(35 µg·m-3),表明西安市采暖季 过渡期空气污染较为严重.与非污染期相比,污染 事件中各化学组分的贡献率有不同程度地增加或减 少, 其中增幅最大的为 SIA(108.0%~243.7%, 事件 I 除外), 其余组分的变化幅度为-36.8%~100.0%. 各污染事件的PM25化学组分也存在一定差异.事件 I中PM25的主要贡献者为OA(贡献率为40.1%)和粉 尘(贡献率为37.9%), 而事件Ⅱ和事件Ⅲ中PM25的 主要贡献者为OA(贡献率分别为31.9%、38.6%)和 SIA(贡献率分别为50.6%、34.8%). 造成这种差异的 原因可能是事件Ⅰ中较高的风速使粉尘浓度增加、 事件Ⅱ中高O。浓度和高相对湿度(RH)为二次组分形 成提供有利条件以及事件Ⅲ初期温度较低,居民取 暖需求增大,生物质燃烧量增加,排放大量的OA. 在不同污染事件中, SIA的浓度均呈现出: NO3> NH4+ > SO2-7, 这可能是由于机动车保有量持续上升 NO<sub>x</sub>排放量增加,清洁能源逐步替代煤炭使得SO<sub>2</sub>排 放量减少[46],从而造成NO3>SO4-.

使用O<sub>x</sub>(O<sub>3</sub>+NO<sub>2</sub>)和RH分别探索OA和SIA在白 天(07:00~18:00)及夜间(19:00至次日06:00)的形 成机制.图2(a)~2(d)描述了观测期间白天OA和 SIA 浓度随  $O_x$  浓度的变化. 当 $\rho(O_x)$  < 70  $\mu g \cdot m^{-3}$  时,  $OA 与 O_x$ 呈显著线性正相关( $R^2 = 0.99, P < 0.01$ ), 其 斜率为 0.51; 当 $\rho$ (O<sub>x</sub>) > 70 μg·m<sup>-3</sup>时, 尽管 OA 与 O<sub>x</sub> 依然呈线性正相关( $R^2 = 0.71$ , P < 0.01), 但其斜率 降至0.13,这可能是受前体物减少影响.对于SIA而 言, SO<sub>4</sub> - 、NO<sub>3</sub> 和 NH<sub>4</sub> + 与 O<sub>x</sub> 整体呈线性正相关(R<sup>2</sup>介 于0.53~0.72),表明光化学氧化反应是上述组分形 成的重要途径.然而它们的斜率差异大,呈现NO:  $(0.16) > NH_4^+(0.06) > SO_4^{2-}(0.03)$ 的特征,表明 NO<sub>3</sub> 的光化学氧化形成速率高于NH<sub>4</sub>+和SO<sub>4</sub>-. 图 2(e)~2 (h)描述了观测期间夜间 OA 和 SIA 浓度随 RH 的变 化. 当RH < 90% 时, OA浓度随RH增加无明显的变 化趋势; 而当RH>90%时, OA浓度显著降低, 这 可能是因为高湿度环境中,气溶胶酸度发生变化, 进而抑制二次有机气溶胶的形成[47,48]. 当RH < 90% 时,SO<sub>4</sub>-、NO<sub>5</sub>和NH<sub>4</sub>-浓度随RH的升高而上升,说 明液相化学反应是夜间 SIA 的重要生成途径;而当 RH > 90% 时,它们浓度显著下降的原因可能是深夜

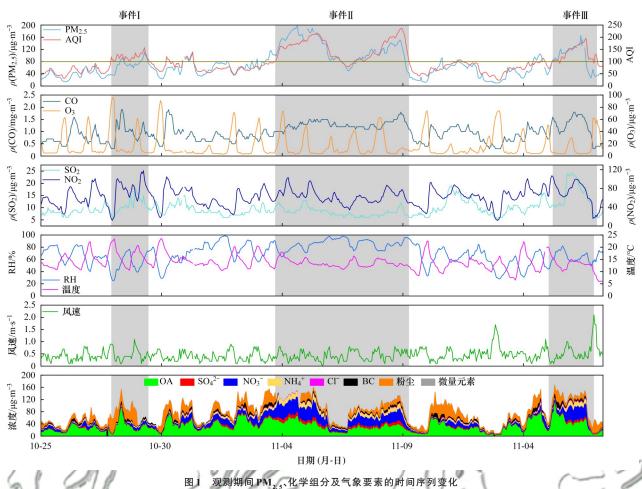


图 I - 观测期间 PM<sub>2:5</sub>、化字组分及气家要素的时间序列受化 Fig. 1 - Time series of PM<sub>2.5</sub>, chemical components and meteorological elements during the observation peri

表 1 不同时期 PM<sub>2.5</sub>化学组分质量浓度/µg·m<sup>-3</sup>

Table 1 Mass concentration of chemical components of PM, 5 in different periods/µg·m<sup>-3</sup>

7.2	整体观	测期间	非污	染期	事件	牛 I	事化	<b>牛Ⅱ</b>	事件	<u></u>
项目	10月25日至 11月17日		除事件Ⅰ、Ⅱ和Ⅲ 外剩余时间		10月28日14:00至10月30日03:00		11月4日09:00至11月9日22:00		11月15日21:00至 11月17日17:00	
4	均值	偏差	均值	偏差	均值	组分	均值	偏差	均值	偏差
$\mathrm{PM}_{2.5}$	78.3	38.5	66.5	34.9	77.3	28.6	96.9	35.1	113.1	39.4
OA	30.3	17.9	28.2	17.5	31.0	19.2	30.9	14.0	43.7	23.9
SO <sub>4</sub> <sup>2-</sup>	4.0	3.1	2.5	1.2	1.9	0.5	7.9	3.2	5.2	2.8
$NO_3^-$	14.9	13.7	8.7	6.9	5.6	3.6	29.9	13.3	25.1	17.3
$NH_4^+$	5.8	4.8	3.6	2.3	2.7	1.2	11.2	4.7	9.1	5.9
Cl <sup>-</sup>	1.0	0.8	0.9	0.9	0.7	0.6	1.0	0.5	1.8	1.0
BC	4.5	3.2	4.4	3.2	5.0	2.7	4.0	2.2	6.4	4.8
粉尘	16.6	13.6	17.1	13.3	29.3	21.9	10.8	8.6	19.9	9.5
微量元素	1.2	0.7	1.1	0.6	1.1	0.8	1.2	0.7	1.9	0.5

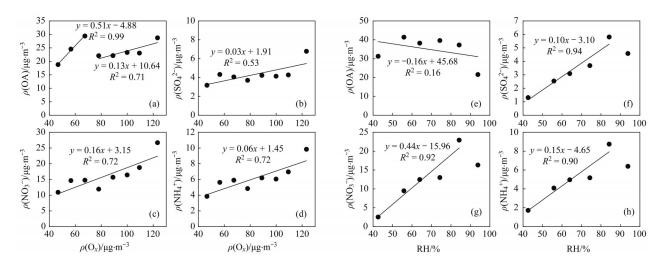
前体物浓度较低,并且RH较高时的吸湿增长也将引发颗粒物沉降<sup>[49]</sup>.

#### 2.2 PM25来源解析

使用PMF解析观测期间PM<sub>25</sub>的来源,基于各化学组分特征确定了6个来源,分别为二次源、生物质燃烧源、扬尘源、机动车源、工业源及燃煤源.图 3 显示了PM<sub>25</sub>的源谱特征及其来源贡献.

因子1中 $NO_3$ 、 $NH_4$ +和 $SO_4$ -的贡献率较高.有研

究表明 NO<sub>3</sub>和 SO<sub>4</sub><sup>2</sup>-主要由其前体物(NO<sub>4</sub>、SO<sub>2</sub>)通过 光化学氧化或液相化学反应生成<sup>[38]</sup>. 因此,将该因 子定义为二次源,其对 PM<sub>2.5</sub>平均贡献率为 29.1%. 因 子 2 中 Cl<sup>-</sup>、BC 和 OA 贡献率较高,这些组分通常来 自生物质燃烧<sup>[50]</sup>. 将该因子定义为生物质燃烧源, 其对 PM<sub>2.5</sub>的贡献率仅次于二次源,为 21.1%. 因子 3 中贡献率较高的组分包括 Si 和 Ca 以及 Ni 和 K 等贡献 率较低的组分. 其中,Si 和 Ca 是典型的地壳元



(a)~(d) 白天 OA 及 SIA 随 O<sub>x</sub> 的变化趋势, (e)~(h) 夜间 OA 及 SIA 随 RH 的变化趋势

#### 图 2 OA及 SIA 随 O、及 RH 变化趋势

Fig. 2 Variation trend of OA and SIA with O, and RH

素[51,52], 而 Ni 和 K 等其他组分也可通过富集因子的 计算(0.27~1.45)判定其主要来自地壳.因此,该因 子定义为扬尘源,其对PM25平均贡献率为15.3%.因 子4中Zn、Mn、Cu和Fe贡献率较高,其中Zn是车 辆润滑油的主要添加剂[38],并且也可作为轮胎橡胶 的硫化活性剂,在车辆行驶中会摩擦产生Zn<sup>[53]</sup>;Cu 用于制作刹车片,车辆刹车摩擦会释放Cu; Fe和 Mn则来自车辆零件腐蚀及制动磨损 [54]. 因此,将该 因子定义为机动车源, 其对 PM25 平均贡献率为 12.9%. 因子 5 中 Co 贡献率最高,此外 Ca、Fe、Mn 和 Cr 等金属元素也有一定的贡献率. Co 主要来自于 与工业相关的煤炭燃烧[55], Cr是冶金工业的重要示 踪物[56]. 将该因子定义为工业源, 其对PM25平均贡 献率为11.4%. As和Se作为典型的煤炭燃烧指示 物[12, 15], 在因子6中贡献率较高,将该因子定义为 燃煤源, 其对 PM<sub>25</sub>贡献率为 10.2%.

不同时期的 PM<sub>25</sub>来源贡献如图 4 所示(事件 I 和事件 II 部分时间段的 PM<sub>25</sub>来源由于缺少元素数据无法解析). 非污染期 PM<sub>25</sub>主要来自生物质燃烧源和二次源,分别贡献了 29.1%(19.2 μg·m<sup>-3</sup>)和 20.5%(13.6 μg·m<sup>-3</sup>);扬尘源、机动车源和工业源贡献率相对较低,分别为 18.4%(12.1 μg·m<sup>-3</sup>)、15.1%(10.0 μg·m<sup>-3</sup>)和 12.7%(8.4 μg·m<sup>-3</sup>);燃煤源贡献率则最低,仅占 4.2%(2.8 μg·m<sup>-3</sup>). 与非污染期相比(事件 I 除外),二次源成为污染期 PM<sub>25</sub>的主要来源,这与其他城市污染期 PM<sub>25</sub>来源结果一致<sup>[57, 58]</sup>;由于居民取暖需求增大,生物质和煤炭消耗量增加,导致生物质燃烧源与燃煤源贡献增加;此外,污染期间工业源、机动车源和扬尘源对 PM<sub>25</sub>的贡献均相对较低.不同事件间 PM<sub>25</sub>的来源贡献也存在着一定的差异,扬尘源作为主要贡献者在事件 I 中的贡献率

(浓度)为38.3%(31.5  $\mu$ g·m<sup>-3</sup>),事件  $\Pi$  和事件  $\Pi$  的主要贡献者二次源的贡献率(浓度)分别为48.1%(45.2  $\mu$ g·m<sup>-3</sup>)和36.1%(39.7  $\mu$ g·m<sup>-3</sup>),此外一次源在3次事件中的贡献率(浓度)分别为96.3%(79.2  $\mu$ g·m<sup>-3</sup>)、51.9%(48.8  $\mu$ g·m<sup>-3</sup>)和63.9%(70.1  $\mu$ g·m<sup>-3</sup>),这表明污染期间  $PM_{25}$ 更多的来自于一次源直接排放,应加大对其的管控.

### 2.3 不同污染事件成因

为了对污染事件进行完整分析,将污染的积累和消散阶段包括在内,重新划分后的污染事件时间段为事件 I: 10月28日08:00至10月30日14:00;事件 II: 11月3日17:00至11月10日08:00;事件 II: 11月15日17:00至11月17日20:00.由于仪器原因事件 I 和事件 II 前半段缺少部分元素数据,考虑到组分数据和来源解析结果的完整性,故只对事件 II 后半段(11月7日08:00至11月10日08:00)及事件 III 进行分析.图 5 展示了事件 II 和事件 III 中化学组分、来源贡献、气态污染物及气象条件的时间序列变化.

根据 AQI 将事件 II 分为 3 个阶段: 11 月 7 日 08:00~15:00 为污染发展阶段(AQI < 100),11 月 7 日 16:00 至 11 月 9 日 15:00 为污染维持阶段(AQI > 100),11 月 9 日 16:00 至 11 月 10 日 08:00 为污染消散阶段(AQI 到达峰值后持续降低). 污染发展阶段 PM<sub>25</sub>以 8.2  $\mu$ g·(m³·h)¬¹的速率上升,各组分浓度大幅增加(BC和微量元素除外). 由于 Ox浓度升高,大气氧化性增强[41],SOR 和 NOR 随之升高,与污染发展阶段相比,污染维持阶段的 $\rho$ (SO<sup>2</sup><sub>4</sub>¬)、 $\rho$ (NO<sup>3</sup><sub>3</sub>)和 $\rho$ (NH<sub>4</sub>+)分别从 5.9、17.5 和 6.7  $\mu$ g·m¬³增加至 8.2、29.2 和 11.5  $\mu$ g·m¬³,同时 $\rho$ (OA)也从 18.9  $\mu$ g·m¬³增加至 28.8  $\mu$ g·m¬³. 受不利气象条件影响, $\rho$ (PM<sub>25</sub>)逐

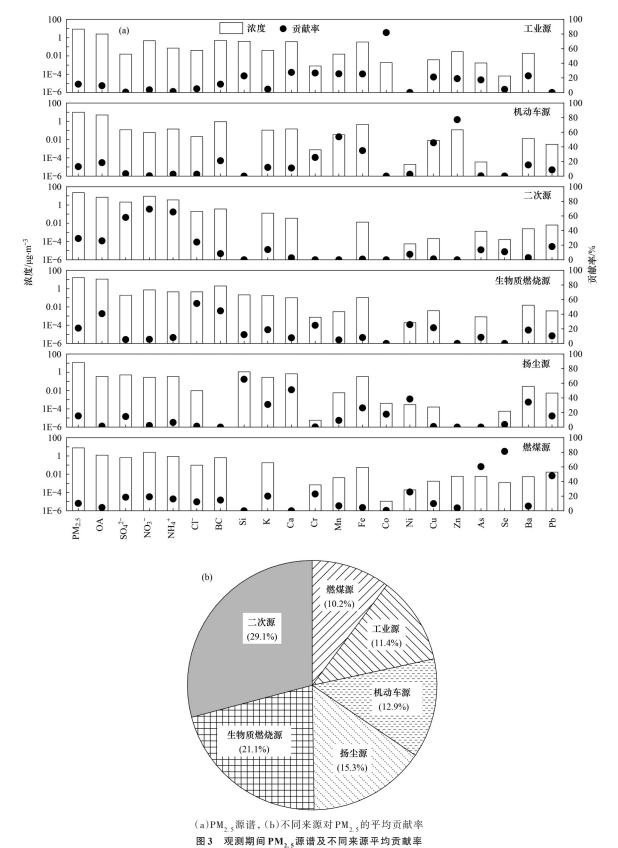


Fig. 3 PM<sub>2,5</sub> source profiles and average contribution rates from different sources during the observation period

渐增加并于 11 月 9 日 11:00 达到此次事件的峰值 (133.2  $\mu$ g·m<sup>-3</sup>). 在高位持续 3 h后,降雨及较高的风速使此次事件进入污染消散阶段,AQI在 11 月 9 日 23:00下降至 100 以下, $\rho$ (PM<sub>25</sub>)维持在 20.0~40.0

μg·m<sup>-3</sup>,与该事件最初相比,粉尘贡献率增加,SIA 组分贡献率降低.通过对比不同阶段各污染源浓度 的变化可以发现,二次源在污染发展和维持阶段是 主要贡献者,其贡献率在50.0%左右;污染维持阶

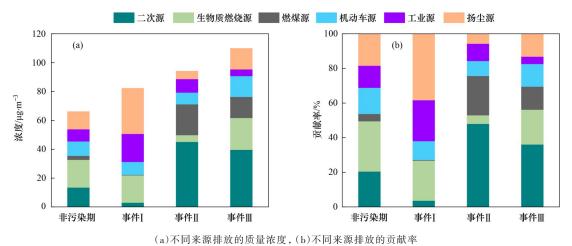


图 4 不同时期不同来源对 PM, 5 的贡献率

Fig. 4 Contribution rates to  $PM_{2.5}$  from different sources at different periods

段生物质燃烧源、燃煤源和工业源的浓度明显高于污染发展阶段;在污染消散阶段随着 PM<sub>2.5</sub>浓度的逐渐降低,除扬尘源浓度逐渐增加外,其余源浓度均呈现下降趋势.这与不同阶段的 O<sub>2</sub>浓度、风速和降雨等气象条件有关.

使用与事件Ⅱ相同的标准对事件Ⅲ进行阶段划

分: 11 月 15 日 17:00 ~ 20:00 为污染发展阶段 (AQI < 100), 11 月 15 日 21:00 至 11 月 17 日 06:00 为污染维持阶段(AQI > 100), 11 月 17 日 07:00~20:00 为污染消散阶段(AQI到达峰值后持续降低). 受集中供暖影响,事件Ⅲ污染程度相对于事件Ⅱ更为严重.污染发展阶段 PM<sub>25</sub>以 18.2 μg·(m³·h)¹的速率上

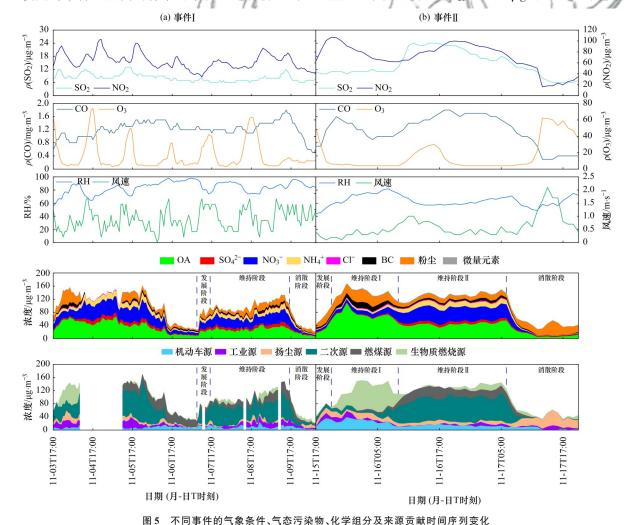


Fig. 5 Change in meteorological conditions, gaseous pollutants, chemical components and source contribution time series of different events

升,其中OA和粉尘是PM25的主要化学组分,其浓 度大幅增加,分别为最初的3.5倍和2.5倍.污染维 持阶段 PM25 化学组成变化较大,将其分为阶段 I (11月15日21:00至11月16日08:00)和阶段Ⅱ(11 月 16 日 09:00 至 11 月 17 日 06:00) 进行讨论. 由于夜 间温度持续下降,居民取暖需求增加使得生物质消 耗量增加,排放大量OA使其成为阶段I中PM25的 主要化学组分(贡献率为52.1%),加之夜间边界层 高度降低导致污染物不易扩散 $^{[59,60]}$ ,使得 $\rho(PM_{2.5})$ 在 11月15日23:00达到此次事件峰值(167.8 μg·m<sup>-3</sup>). 受夜间液相化学、日间光化学氧化反应及静稳天气 条件影响, SIA 组分浓度持续增加, 阶段 Ⅱ中 PM25 的主要化学组分由 OA 转变为 SIA 组分(贡献率为 49.1%),但SIA组分浓度与事件Ⅱ污染维持阶段相 比较低,其原因在于事件Ⅱ有着更高的Ox浓度和 RH, 为气态前体物的二次转化提供有利条件.11月 17日07:00开始进入此次事件的污染消散阶段,由 于风速的持续升高使得污染物逐渐扩散[61],与事件 Ⅱ类似,粉尘组分浓度持续增加并成为该阶段PM25 的主要化学组分(贡献率为57.8%),其余化学组分 浓度均持续下降,  $\rho(PM_{25})$ 降至 40.0  $\mu g \cdot m^{-3}$ 左右. 通 过图5可以看出此次事件不同阶段的各污染源浓度 变化较大,与事件Ⅱ不同的是在污染发展阶段,机 动车源是PM25的主要贡献者,这可能是晚高峰所 致;生物质燃烧源和二次源则分别是污染维持阶段 I 和阶段 II 中 PM₂₅的主要贡献者,这与事件 II 也存 在着一定差异,主要是受取暖强度的影响;污染消 散阶段与事件Ⅱ相同, PM25的主要贡献者为扬尘源.

#### 3 结论

- (1) 观测期间  $\rho$  (PM<sub>2.5</sub>) 平均值为 (78.3 ± 38.5)  $\mu$ g·m<sup>-3</sup>,高于环境空气质量一级标准,表明该时期空气污染较为严重. 观测期间 PM<sub>2.5</sub>的主要化学组分为 OA(贡献率为 38.7%)、SIA(贡献率为 31.6%)和粉尘(贡献率为 21.2%),BC(贡献率为 5.7%)、CI-(贡献率为 1.3%)及微量元素(贡献率为 1.5%)对 PM<sub>2.5</sub>贡献率相对较低. OA 和 SIA 与 O<sub>2</sub> 的相关性表明光化学氧化反应是其形成的重要途径;同时在 RH 低于90%时,SIA 与 RH 密切相关,反映了液相化学反应的重要性.
- (2)基于高时间分辨率组分数据,使用PMF模型确定了PM<sub>25</sub>的6个来源,分别为二次源(贡献率为29.1%)、生物质燃烧源(贡献率为21.1%)、扬尘源(贡献率为15.3%)、机动车源(贡献率为12.9%)、工业源(贡献率为11.4%)和燃煤源(贡献率为10.2%).非污染期PM<sub>25</sub>主要来自生物质燃烧源和扬尘源,二

次源成为污染期间 PM<sub>25</sub>的主要来源(事件 I 为扬 尘源).

(3)两次事件中污染维持阶段 PM<sub>25</sub>的主要化学组分为 OA 和 SIA 组分,消散阶段为粉尘组分.受取暖需求影响,事件Ⅲ中污染维持阶段 I 的 PM<sub>25</sub>主要来源为生物质燃烧源,污染维持阶段 Ⅱ 与事件 Ⅱ 相同,为二次源,污染消散阶段扬尘源则成为 PM<sub>25</sub>的主要来源.

#### 参考文献:

- [ 1 ] Lelieveld J, Evans J S, Fnais M, et al. The contribution of outdoor air pollution sources to premature mortality on a global scale [J]. Nature, 2015, 525(7569): 367-371.
- [2] Hu J L, Ying Q, Wang Y G, et al. Characterizing multi-pollutant air pollution in China: comparison of three air quality indices [J]. Environment International, 2015, 84: 17-25.
- [ 3 ] Lin H L, Liu T, Xiao J P, et al. Mortality burden of ambient fine particulate air pollution in six Chinese cities: results from the Pearl River Delta study [J]. Environment International, 2016, 96: 91-97.
- [4] Zhu Y H, Huang L, Li J Y, et al. Sources of particulate matter in China: insights from source apportionment studies published in 1987-2017 [J]. Environment International, 2018, 115: 343-357.
- [5] Saha M, Maharana D, Kurumisawa R, et al. Seasonal trends of atmospheric PAHs in five Asian megacities and source detection using suitable biomarkers [J]. Aerosol and Air Quality Research, 2017, 17(9): 2247-2262.
- [6] Li F X, Gu J W, Xin J Y, et al. Characteristics of chemical profile, sources and PAH toxicity of PM<sub>2.5</sub> in beijing in autumnwinter transit season with regard to domestic heating, pollution control measures and meteorology [J]. Chemosphere, 2021, 276, doi: 10.1016/j.chemosphere.2021.130143.
- [7] Wang H, Wang S L, Zhang J Q, et al. Characteristics of PM<sub>2.5</sub> pollution with comparative analysis of O<sub>3</sub> in Autumn Winter seasons of Xingtai, China[J]. Atmosphere, 2021, 12(5), doi: 10. 3390/atmos12050569.
- [8] Yang S, Duan F K, Ma Y L, et al. Mixed and intensive haze pollution during the transition period between autumn and Winter in Beijing, China[J]. Science of the Total Environment, 2020, 711, doi: 10.1016/j.scitotenv.2019.134745.
- [9] 李明燕, 杨文,魏敏,等.典型沿海城市采暖期细颗粒物组分特征及来源解析[J]. 环境科学, 2020, 41(4): 1550-1560. Li M Y, Yang W, Wei M, et al. Characteristics and sources apportionment of fine particulate matter in a typical coastal city during the heating period [J]. Environmental Science, 2020, 41 (4): 1550-1560.
- [10] 朱淑贞, 佟洁, 鲍丰, 等. 廊坊市秋冬季大气细颗粒物污染特征及来源解析[J]. 环境科学, 2023, 44(1): 20-29.

  Zhu S Z, Tong J, Bao F, et al. Characteristics and source apportionment of atmospheric fine particles in Langfang in autumn and winter[J]. Environmental Science, 2023, 44(1): 20-29.
- [11] 路娜,李治国,周静博,等.2015年石家庄市采暖期一次重污染过程细颗粒物在线来源解析[J].环境科学,2017,38(3):884-893.
  - Lu N, Li Z G, Zhou J B, et al. Online source analysis of particulate matter ( $PM_{2.5}$ ) in a heavy pollution process of Shijiazhuang city during heating period in 2015 [J]. Environmental Science, 2017, 38(3): 884-893.

- [12] Liu Y F, Li C L, Zhang C, et al. Chemical characteristics, source apportionment, and regional contribution of PM<sub>2.5</sub> in Zhangjiakou, Northern China: a multiple sampling sites observation and modeling perspective[J]. Environmental Advances, 2021, 3, doi: 10.1016/j.envadv.2021.100034.
- [13] Gao J, Peng X, Chen G, et al. Insights into the chemical characterization and sources of PM<sub>2.5</sub> in Beijing at a 1-h time resolution [J]. Science of the Total Environment, 2016, 542: 162-171
- [14] Sun Y L, Wang Z F, Du W, et al. Long-term real-time measurements of aerosol particle composition in Beijing, China: seasonal variations, meteorological effects, and source analysis[J]. Atmospheric Chemistry and Physics, 2015, 15 (17): 10149-10165.
- [15] Shen J Y, Zhao Q B, Cheng Z, et al. Evolution of source contributions during heavy fine particulate matter (PM<sub>2.5</sub>) pollution episodes in Eastern China through online measurements [J]. Atmospheric Environment, 2020, 232, doi: 10.1016/j.atmosenv. 2020.117569.
- [16] Pang N N, Gao J, Che F, et al. Cause of PM<sub>2.5</sub> pollution during the 2016-2017 heating season in Beijing, Tianjin, and Langfang, China [1]. Journal of Environmental Sciences, 2020, 95: 201-209.
- [17] Han S Q, Wu J H, Zhang Y F, et al. Characteristics and formation mechanism of a winter haze - fog episode in Tianjin, China [J]. Atmospheric Environment, 2014, 98; 323-330.
- [18] Lv L L, Chen Y J, Han Y, et al. High-time-resolution PM<sub>2.5</sub> source apportionment based on multi-model with organic tracers in Beijing during haze episodes [J]. Science of the Total Environment, 2021, 772, doi: 10.1016/j.scitotenv.2020.144766.
- [19] Cheng J, Tong D, Liu Y, et al. Air quality and health benefits of China's current and upcoming clean air policies [J]. Faraday Discussions, 2021, 226: 584-606.
- [20] 李雁宇, 李杰, 曾胜兰, 等. 2017年汾渭平原东部大气颗粒物污染特征分析[J]. 环境科学研究, 2020, 33(1): 63-72. Li Y Y, Li J, Zeng S L, et al. Analysis of atmospheric particulates in the eastern Fenwei Plain in 2017[J]. Research of Environmental Sciences, 2020, 33(1): 63-72.
- [21] Dao X, Ji D S, Zhang X, et al. Characteristics, sources and health risk assessment of PM<sub>25</sub> in China's coal and coking heartland: insights gained from the regional observations during the heating season[J]. Atmospheric Pollution Research, 2021, 12(12), doi: 10.1016/j.apr.2021.101237.
- [22] Liu Y, Xu X J, Yang X Y, et al. Significant contribution of secondary particulate matter to recurrent air pollution: evidence from in situ observation in the most polluted city of Fen-Wei Plain of China [J]. Journal of Environmental Sciences, 2022, 114: 422-433.
- [23] Li Y F, Liu B S, Xue Z G, et al. Chemical characteristics and source apportionment of PM<sub>2.5</sub> using PMF modelling coupled with 1hr resolution online air pollutant dataset for Linfen, China [J]. Environmental Pollution, 2020, 263, doi: 10.1016/j.envpol.2020. 114532.
- [24] 李慧,王涵,严沁,等. 汾渭平原秋冬季 PM<sub>25</sub>化学组分特征及 其来源[J]. 环境科学研究, 2023, **36**(3): 449-459. Li H, Wang H, Yan Q, *et al.* Chemical composition characteristics and source apportionment of PM<sub>25</sub> in the Fenwei Plain in autumn and winter [J]. Research of Environmental Sciences, 2023, **36** (3): 449-459.
- [25] Liu X D, Hui Y, Yin Z Y, et al. Deteriorating haze situation and the severe haze episode during December 18 - 25 of 2013 in Xi'an,

- China, the worst event on record [J]. Theoretical and Applied Climatology, 2016, 125(1-2): 321-335.
- [26] Wang P, Cao J J, Shen Z X, et al. Spatial and seasonal variations of PM<sub>2.5</sub> mass and species during 2010 in Xi'an, China[J]. Science of the Total Environment, 2015, 508: 477-487.
- [27] Zhang T, Cao J J, Tie X X, et al. Water-soluble ions in atmospheric aerosols measured in Xi'an, China: seasonal variations and sources [J]. Atmospheric Research, 2011, 102(1-2): 110-119.
- [28] Zhang T, Shen Z X, Su H, et al. Effects of aerosol water content on the formation of secondary inorganic aerosol during a winter heavy PM<sub>2.5</sub> pollution episode in Xi 'an, China [J]. Atmospheric Environment, 2021, 252, doi: 10.1016/j.atmosenv.2021.118304.
- [29] Dai Q L, Bi X H, Liu B S, et al. Chemical nature of PM<sub>25</sub> and PM<sub>10</sub> in Xi an, China: insights into primary emissions and secondary particle formation [J]. Environmental Pollution, 2018, 240: 155-166.
- [30] Wang X, Shen Z X, Liu F B, et al. Saccharides in summer and winter PM<sub>2.5</sub> over Xi'an, Northwestern China: sources, and yearly variations of biomass burning contribution to PM<sub>2.5</sub>[J]. Atmospheric Research, 2018, 214: 410-417.
- [31] Liu P P, Lei Y L, Ren H R, et al. Seasonal variation and health risk assessment of heavy metals in PM<sub>2.5</sub> during winter and summer over Xi'an, China[J]. Atmosphere, 2017, 8(5), doi: 10.3390/ atmos8050091.
- [32] Tian J, Wang Q Y, Zhang Y, et al. Impacts of primary emissions and secondary aerosol formation on air pollution in an urban area of China during the COVID-19 lockdown [J]. Environment International, 2021, 150, doi: 10.1016/j.envint.2021.106426.
- [33] Rajesh T A, Ramachandran S. Black carbon aerosol mass concentration, absorption and single scattering albedo from single and dual spot aethalometers: radiative implications [J]. Journal of Aerosol Science, 2018, 119: 77-90.
- [34] Drinovec L, Močnik G, Zotter P, et al. The "dual-spot" aethalometer: an improved measurement of aerosol black carbon with real-time loading compensation[J]. Atmospheric Measurement Techniques, 2015, 8(5): 1965-1979.
- [35] Zhao S, Tian H Z, Luo L N, et al. Temporal variation characteristics and source apportionment of metal elements in PM<sub>2.5</sub> in urban Beijing during 2018-2019[J]. Environmental Pollution, 2021, 268, doi: 10.1016/j.envpol.2020.115856.
- [36] Furger M, Minguillón M C, Yadav V, et al. Elemental composition of ambient aerosols measured with high temporal resolution using an online XRF spectrometer [J]. Atmospheric Measurement Techniques, 2017, 10(6): 2061-2076.
- [37] Chow J C, Lowenthal D H, Chen L W A, et al. Mass reconstruction methods for PM<sub>25</sub>: a review [J]. Air Quality, Atmosphere & Health, 2015, 8(3): 243-263.
- [38] Srivastava D, Xu J S, Vu T V, et al. Insight into PM<sub>25</sub> sources by applying positive matrix factorization (PMF) at urban and rural sites of Beijing[J]. Atmospheric Chemistry and Physics, 2021, 21 (19): 14703-14724.
- [39] Xu X M, Zhang H F, Chen J M, et al. Six sources mainly contributing to the haze episodes and health risk assessment of PM<sub>2.5</sub> at Beijing suburb in winter 2016 [J]. Ecotoxicology and Environmental Safety, 2018, 166: 146-156.
- [40] Xu Q C, Wang S X, Jiang J K, et al. Nitrate dominates the chemical composition of PM<sub>2.5</sub> during haze event in Beijing, China [J]. Science of the Total Environment, 2019, 689: 1293-1303.
- [41] Xie Y Z, Liu Z R, Wen T X, et al. Characteristics of chemical

- composition and seasonal variations of  $PM_{25}$  in Shijiazhuang, China: impact of primary emissions and secondary formation [J]. Science of the Total Environment, 2019, **677**: 215-229.
- [42] Sun Y L, Zhuang G S, Tang A H, et al. Chemical characteristics of PM<sub>2.5</sub> and PM<sub>10</sub> in haze-fog episodes in Beijing [J]. Environmental Science & Technology, 2006, 40(10): 3148-3155.
- [43] Hopke P K. Review of receptor modeling methods for source apportionment [J]. Journal of the Air & Waste Management Association, 2016, 66(3): 237-259.
- [44] Han F L, Kota S H, Wang Y G, et al. Source apportionment of PM<sub>2.5</sub> in Baton Rouge, Louisiana during 2009-2014[J]. Science of the Total Environment, 2017, 586: 115-126.
- [45] Belis C A, Pikridas M, Lucarelli F, et al. Source apportionment of fine PM by combining high time resolution organic and inorganic chemical composition datasets [J]. Atmospheric Environment: X, 2019, 3, doi: 10.1016/j.aeaoa.2019.100046.
- [46] Li R, Cui L L, Li J L, et al. Spatial and temporal variation of particulate matter and gaseous pollutants in China during 2014 -2016[J]. Atmospheric Environment, 2017, 161: 235-246.
- [47] Huang X J, Zhang J K, Luo B, et al. Characterization of oxalic acid-containing particles in summer and winter seasons in Chengdu, China [J]. Atmospheric Environment, 2019, 198: 133-141.
- [48] Meng J J, Wang G H, Li J J, et al. Seasonal characteristics of oxalic acid and related SOA in the free troposphere of Mt. Hua, Central China: implications for sources and formation mechanisms [J]. Science of the Total Environment, 2014, 493: 1088-1097.
- [49] Chen Z Y, Chen D L, Zhao C F, et al. Influence of meteorological conditions on PM<sub>2.5</sub> concentrations across China; a review of methodology and mechanism [J]. Environment International, 2020, 139, doi: 10.1016/j.envint.2020.105558.
- [50] Cesari D, Donateo A, Conte M, et al. An inter-comparison of PM<sub>2.5</sub> at urban and urban background sites: chemical characterization and source apportionment[J]. Atmospheric Research, 2016, 174-175: 106-119.
- [51] Rai P, Furger M, Slowik J G, et al. Characteristics and sources of hourly elements in PM<sub>10</sub> and PM<sub>2.5</sub> during wintertime in Beijing[J]. Environmental Pollution, 2021, 278, doi: 10.1016/j.envpol.2021. 116865.
- [52] Zhou S Z, Davy P K, Huang M J, et al. High-resolution sampling and analysis of ambient particulate matter in the Pearl River Delta region of Southern China: source apportionment and health risk

- implications [J]. Atmospheric Chemistry and Physics, 2018, 18 (3) · 2049-2064.
- [53] Li M L, Liu Z R, Chen J, et al. Characteristics and source apportionment of metallic elements in PM<sub>2.5</sub> at urban and suburban sites in Beijing: implication of emission reduction [J]. Atmosphere, 2019, 10(3), doi: 10.3390/atmos10030105.
- [54] Piscitello A, Bianco C, Casasso A, et al. Non-exhaust traffic emissions: sources, characterization, and mitigation measures [J]. Science of the Total Environment, 2021, 766, doi: 10.1016/j. scitotenv.2020.144440.
- [55] Chen Y, Xie S D, Luo B, et al. Particulate pollution in urban Chongqing of southwest China: historical trends of variation, chemical characteristics and source apportionment [J]. Science of the Total Environment, 2017, 584-585: 523-534.
- [56] Dall'Osto M, Booth M J, Smith W, et al. A study of the size distributions and the chemical characterization of airborne particles in the vicinity of a large integrated steelworks [J]. Aerosol Science and Technology, 2008, 42(12): 981-991.
- [57] 刘倬诚, 牛月圆, 吴婧, 等. 山地型城市冬季大气重污染过程特征及成因分析[J]. 环境科学, 2021, 42(3): 1306-1314.

  Liu Z C, Niu Y Y, Wu J, et al. Characteristics and cause analysis of heavy air pollution in a mountainous city during winter [J]. Environmental Science, 2021, 42(3): 1306-1314.
- [58] 夏丽,朱彬,王红磊,等.长三角地区一次区域污染过程中细颗粒物的来源解析及其光学特性[J].环境科学,2021,42 (2):556-563.

  Xia L, Zhu B, Wang H L, et al. Source apportionment and optical properties of fine particles associated with regional pollution in the Yangtze River Delta [J]. Environmental Science, 2021, 42 (2):556-563.
- [59] Zhu W H, Xu X D, Zheng J, et al. The characteristics of abnormal wintertime pollution events in the Jing-Jin-Ji region and its relationships with meteorological factors [J]. Science of the Total Environment, 2018, 626: 887-898.
- [60] Liu N, Zhou S, Liu C S, et al. Synoptic circulation pattern and boundary layer structure associated with PM<sub>2.5</sub> during wintertime haze pollution episodes in Shanghai [J]. Atmospheric Research, 2019, 228: 186-195.
- [61] Zhang L Y, Cheng Y, Zhang Y, et al. Impact of air humidity fluctuation on the rise of PM mass concentration based on the highresolution monitoring data [J]. Aerosol and Air Quality Research, 2017, 17(2): 543-552.

# **HUANJING KEXUE**

Environmental Science (monthly)

Vol. 45 No. 5 May 15, 2024

## **CONTENTS**

CONTENTS	
Spatial Distribution Characteristics of PM <sub>2,5</sub> and O <sub>3</sub> in Beijing-Tianjin-Hebei Region Based on Time Series Decomposition	YAO Qing, DING Jing, YANG Xu, et al. (2487)
Ozone Sensitivity Analysis in Urban Beijing Based on Random Forest	
Prediction of Ozone Pollution in Sichuan Basin Based on Random Forest Model	····YANG Xiao-tong, KANG Ping, WANG An-yi, et al. (2507)
Establishment and Effective Evaluation of Haikou Ozone Concentration Statistical Prediction Model	···FU Chuan-bo, LIN Jian-xing, TANG Jia-xiang, et al. (2516)
Spatial and Temporal Distribution Characteristics of Ozone Concentration and Health Benefit Assessment in the Beijing-Tianjin-Hebei Re	egion from 2015 to 2020
7	
Water-soluble Inorganic Ion Content of PM <sub>2.5</sub> and Its Change Characteristics in Urban Area of Beijing in 2022·····	
Pollution Characteristics, Source, and Health Risk Assessment of Metal Elements in PM <sub>2.5</sub> Between Winter and Spring in Zhengzhou ·····	
Characteristics, Sources Apportionment, and Health Risks of PM <sub>2.5</sub> -bound PAHs and Their Derivatives Before and After Heating in Zibo	CitySUN Gang-li, WU Li-ping, XU Bo, et al. (2558)
Components Characteristic and Source Apportionment of Fine Particulate Matter in Transition Period of Heating Season in Xi'an with High	Time Resolution
Source and Cause Analysis of High Concentration of Inorganic Aerosol During Two Typical Pollution Processes in Winter over Tianjin	<u>.</u>
Spatial-temporal Variation and Spatial Differentiation Geographic Detection of PM <sub>2.5</sub> Concentration in the Shandong Province Based on Sp	atial Scale Effect
1 1 01 23	
Characteristics of VOCs Emissions and Ozone Formation Potential for Typical Chemicals Industry Sources in China	
Formation Potential of Secondary Organic Aerosols and Sources of Volatile Organic Compounds During an Air Pollution Episode in Autum	n , Langfang
	·ZHANG Jing-qiao, LIU Zheng, DING Wen-wen, et al. (2622)
Scale Effects of Landscape Pattern on Impacts of River Water Quality: A Meta-analysis	
Spectral Characteristics and Sources of Dissolved Organic Matter in Inflow Rivers of Baiyangdian Lake Water in Summer Flood Season  Analysis on Hydrochemical Evolution of Shallow Groundwater East of Yongding River in Fengtai District, Beijing	
	• •
Hydrochemical Characteristics, Controlling Factors and Water Quality Evaluation of Shallow Groundwater in Tan-Lu Fault Zone (Anhui S Effects of Pesticides Use on Pesticides Residues and Its Environmental Risk Assessment in Xingkai Lake (China)	
Characteristics of Microorganisms and Antibiotic Resistance Genes of the Riparian Soil in the Lanzhou Section of the Yellow River	
Analysis of the Spatiotemporal Distribution of Algal Blooms and Its Driving Factors in Chaohu Lake Based on Multi-source Datasets	
Characteristics of Epiphytic Bacterial Community on Submerged Macrophytes in Water Environment Supplemented with Reclaimed Water	
Effects of Water Level Fluctuations and Vegetation Restoration on Soil Prokaryotic Microbial Community Structure in the Riparian Zone of	V .
Effects of ward 12001 includations and vegetation restolation on John Howaryone sincional community Studente in the repartant zone of	
Bacterial Community Structure of Typical Lake Sediments in Yinchuan City and Its Response to Heavy Metals	
Effect of Thermal Hydrolysis Pretreatment Time on Microbial Community Structure in Sludge Anaerobic Digestion System	
Source Apportionment of Morphine in Wastewater	
Ecological Environment Dynamical Evaluation of Hutuo River Basin Using Remote Sensing	
Spatiotemporal Evolution and Influencing Factors of Ecosystem Service Value in the Yellow River Basin	
Ecosystem Service Trade-off Synergy Strength and Spatial Pattern Optimization Based on Bayesian Network: A Case Study of the Fenhe R	iver Basin
	CAI Jin, WEI Xiao-jian, JIANG Ping, et al. (2780)
Spatial-temporal Evolution and Quantitative Attribution of Habitat Quality in Typical Karst Counties of Guizhou Plateau	LI Yue, FENG Xia, WU Lu-hua, et al. (2793)
Spatio-temporal Variation in NEP in Ecological Zoning on the Loess Plateau and Its Driving Factors from 2000 to 2021	
Land Change Simulation and Grassland Carbon Storage in the Loess Plateau Based on SSP-RCP Scenarios	············CUI Xie, DONG Yan, ZHANG Lu-yin, et al. (2817)
Multi-scenario Simulation of Construction Land Expansion and Its Impact on Ecosystem Carbon Storage in Beijing-Tianjin-Hebei Urban A	Agglomeration
1	
Effects of Land Use Change on Soil Aggregate Stability and Soil Aggregate Organic Carbon in Karst Area of Southwest China	
Integrated Analysis of Soil Organic Matter Molecular Composition Changes Under Different Land Uses	
Prediction Spatial Distribution of Soil Organic Matter Based on Improved BP Neural Network with Optimized Sparrow Search Algorithm	
Effects of Application of Different Organic Materials on Phosphorus Accumulation and Transformation in Vegetable Fields	•
Intensive Citrus Cultivation Suppresses Soil Phosphorus Cycling Microbial Activity ZHOU	
Effects of Controlled-release Blended Fertilizer on Crop Yield and Greenhouse Gas Emissions in Wheat-maize Rotation System  Effect of Biochar on NO <sub>3</sub> -N Transport in Loessial Soil and Its Simulation	
Analysis and Evaluation of Heavy Metal Pollution in Farmland Soil in China; A Meta-analysis	
Critical Review on Heavy Metal Contamination in Urban Soil and Surface Dust	
Research Progress on Solidification and MICP Remediation of Soils in Heavy Metal Contaminated Site	
Pollution Characteristics and Source Analysis of Soil Heavy Metal in Coal Mine Area near the Yellow River in Shandong	
Heavy Metal Content and Risk Assessment of Sediments and Soils in the Juma River Basin	
Characteristics, Ecological Risk Assessment, and Source Apportionment of Soil Heavy Metals in the Yellow River Floodplain of Yinchuan	
Health Risk Assessment of Heavy Metals in Soils of a City in Guangdong Province Based on Source Oriented and Monte Carlo Models	
Chemical Speciation, Influencing Factors, and Regression Model of Heavy Metals in Farmland of Typical Carbonate Area with High Geol	ogical Background, Southwest China
	TANG Rui-ling, XU Jin-li, LIU Bin, et al. (2995)
Hg Content Characteristics and Safe Planting Zoning of Paddy Soil and Rice in Guizhou Province	
Cadmium Phytoremediation Effect of Sweet Sorghum Assisted with Citric Acid on Typical Parent Soil in Southern China	······LIU Meng-yu, LUO Xu-feng, GU Jiao-feng, et al. (3016)
Effects of Modified Distillers' Grains Biochar on Cadmium Forms in Purple Soil and Cadmium Uptake by Rice	IAO Nai-chuan, WANG Zi-fang, YANG Wen-na, et al. (3027)
Effects of Biochar on Growth and Pollutant Accumulation of Lettuce in Soil Co-contaminated with Tetracycline and CopperZHE	
Effects of Vermicomposting on Compost Quality and Heavy Metals: A Meta-analysis	
$Advances \ in \ the \ Effects \ of \ Microplastics \ on \ Soil \ N_2O \ Emissions \ and \ Nitrogen \ Transformation \ \cdots$	
Effects of Land Use Patterns on Soil Microplastic Pollution in the Luoshijiang Sub-watershed of Erhai Lake Basin	
Characteristics of Microplastic Pollution in Sediment of Silty Coast in Culture Bay	
Effect of Polyethylene Microplastics on the Microbial Community of Saline Soils	
Characterization of Microplastic Surface Bacterial Community Structure and Prediction of Ecological Risk in Poyang Lake, China	
Energy-saving and Emission Reduction Path for Road Traffic in Key Coastal Cities of Guangdong, Fujian and Zhejiang	
Life Cycle Carbon Reduction Benefits of Electric Heavy-duty Truck to Replace Diesel Heavy-duty TruckXU Yua	nn-yuan, GONG De-hong, HUANG Zheng-guang, et al. (3119)